



**HAL**  
open science

## Upper Paleozoic komatiites near Mashhad, NE Iran

Mohsen Mobasheri, Nicholas Arndt, Carole Cordier, Alexander Sobolev,  
Habibollah Ghasemi, Carlos J. Garrido

► **To cite this version:**

Mohsen Mobasheri, Nicholas Arndt, Carole Cordier, Alexander Sobolev, Habibollah Ghasemi, et al.. Upper Paleozoic komatiites near Mashhad, NE Iran. *Geology*, 2024, 10.1130/G52289.1 . hal-04712040

**HAL Id: hal-04712040**

**<https://hal.science/hal-04712040v1>**

Submitted on 28 Sep 2024

**HAL** is a multi-disciplinary open access archive for the deposit and dissemination of scientific research documents, whether they are published or not. The documents may come from teaching and research institutions in France or abroad, or from public or private research centers.

L'archive ouverte pluridisciplinaire **HAL**, est destinée au dépôt et à la diffusion de documents scientifiques de niveau recherche, publiés ou non, émanant des établissements d'enseignement et de recherche français ou étrangers, des laboratoires publics ou privés.



Distributed under a Creative Commons Attribution 4.0 International License

# Upper Paleozoic komatiites near Mashhad, NE Iran

Mohsen Mobasheri<sup>1,2</sup>, Nicholas Arndt<sup>3,\*</sup>, Carole Cordier<sup>3</sup>, Alexander Sobolev<sup>3</sup>, Habibollah Ghasemi<sup>1,2</sup>, and Carlos J. Garrido<sup>4</sup>

<sup>1</sup>Department of Petrology and Economic Geology, Faculty of Earth Sciences, Shahrood University of Technology, Haft-e-Tir Sq., Shahrood 3619995161, Iran

<sup>2</sup>Section of Earth Science, Zargan Natural Resources and Mineral Industries Research and Consulting Group, Paradise Blvd., Kerman 7614655140, Iran

<sup>3</sup>Institut des Sciences de la Terre (ISTerre), Université Grenoble Alpes, 1381 rue de la Piscine, Saint-Martin-d'Hères, France

<sup>4</sup>Instituto Andaluz de Ciencias de la Tierra (IACT), Consejo Superior de Investigaciones Científicas (CSIC), Av. de las Palmeras 4, 18100 Armilla, Granada, Spain

## ABSTRACT

We report the discovery of upper Paleozoic komatiites from a location near Mashhad in NE Iran. Like Archean komatiites, they erupted as differentiated lava flows with olivine spinifex-textured upper portions and olivine cumulate lower portions. They are associated with komatiitic basalts and undifferentiated ultramafic units and are intercalated with clastic and carbonate sedimentary rocks. Using the compositions of samples with randomly oriented spinifex and the forsterite contents of olivine, we estimate that the parental magmas contained >20 wt% MgO. As such, they represent only the second known occurrence of post-Archean komatiite. Their geochemical compositions show relatively low Al/Ti and depleted heavy rare earth elements, indicating that they belong to the Al-depleted variety. This is the only reported post-Archean example of this type of komatiite. The parental magmas probably formed by moderate degrees of melting (~20%) of a hydrous peridotite source at a depth of ~180 km and erupted into a subduction zone at the margin of the Paleo-Tethys Ocean.

## INTRODUCTION

Komatiites are largely an Archean phenomenon (Nesbitt et al., 1982). Only a single younger example—the komatiites of Gorgona Island, Colombia—has been convincingly documented (Echeverría, 1980; Kerr, 2005). Several occurrences of ultramafic volcanic rocks have been recognized, such as those from Tortugal in Costa Rica (Trela et al., 2017) and Song Da in Vietnam (Hanski et al., 2001, 2004), and although these rocks have been called komatiite, they do not contain macroscopic spinifex texture and are best referred to as picrites. Proterozoic komatiitic basalts with spinifex textures occur on Gilmour Island, Canada (Arndt et al., 1987), but the maximum MgO content in non-cumulus samples is ~17 wt%.

Here we report a new discovery of komatiites of probable Permian age from a location near Mashhad in NE Iran. These rocks contain olivine

spinifex textures with MgO contents ranging from 25 to 37 wt%. Spatially associated komatiitic basalts contain 6–11 wt% MgO in non-cumulus sections. We use the MgO contents of samples with randomly oriented spinifex olivines and the forsterite contents of these olivines to estimate the composition and temperature of the magmas that erupted to form these lavas, and we demonstrate that this magma had an ultramafic composition. This, together with the well-developed olivine spinifex textures, demonstrates that these rocks are true komatiites.

## GEOLOGICAL SETTING AND FIELD FEATURES

The komatiites are located in the Mashhad-Fariman region in NE Iran within two orogenic belts, the Shandiz-Virani-Mashhad Complex and the Fariman Complex (see Fig. S1 and the description in the Supplemental Material<sup>1</sup>). The two orogenic belts are thought to have developed at the margins of the Paleo-Tethys Ocean between the Eurasian plate (Turan plate) in the north and the Iranian Cimmerian microconti-

ment to the south. Ascent of a mantle plume into a late Paleozoic subduction zone at the margin of the Paleo-Tethys Ocean is a possible geodynamic setting for the generation of these komatiites.

Both complexes contain differentiated and undifferentiated komatiite lava flows, komatiitic basaltic lavas, and mafic or ultramafic pillowed units (Mobasheri et al., 2019). The volcanic rocks erupted into a sequence of poorly consolidated shales, sandstones, and carbonaceous sediments, in places resulting in contact metamorphism and mingling of lava with unconsolidated sediment to form peperites. The age of the sequence is estimated on the basis of microfossils (Kozur and Mostler, 1991; Zanchetta et al., 2013) and Ar-Ar geochronology to be ca. 280 Ma or Permian (Ghazi et al., 2001; Topuz et al., 2018).

Some of the komatiite lava flows are differentiated into upper spinifex-textured layers and lower cumulate layers (Fig. 1). These units range in thickness from <10 m to >100 m. They are bounded by upper and lower chilled margins. In the several ultramafic units, a layer of spinifex texture in which olivine crystals are randomly oriented (Figs. 1 and 2) is underlain by platy pyroxene spinifex. In komatiitic basaltic units, the spinifex layer is underlain by gabbro and a thin layer of pyroxene cumulate (Fig. 2A). In almost all cases, the lower part is composed of olivine orthocumulate.

## PETROGRAPHY

Detailed descriptions of all samples, including komatiitic basalts and associated mafic-ultramafic units, are summarized in the Supplemental Material. Here we describe only the komatiites.

Nicholas Arndt  <https://orcid.org/0009-0003-6925-6338>  
\*nicholas.arndt@univ-grenoble-alpes.fr

<sup>1</sup>Supplemental Material. S1—a description of the contents of an article in preparation; S2—analytical methods; Table S1—compositions of olivine; Table S2—compositions of Cr spinel; Table S3—major and trace elements in samples; and Figures S1–S5. Please visit <https://doi.org/10.1130/G52289.1> to access the supplemental material; contact editing@geosociety.org with any questions.

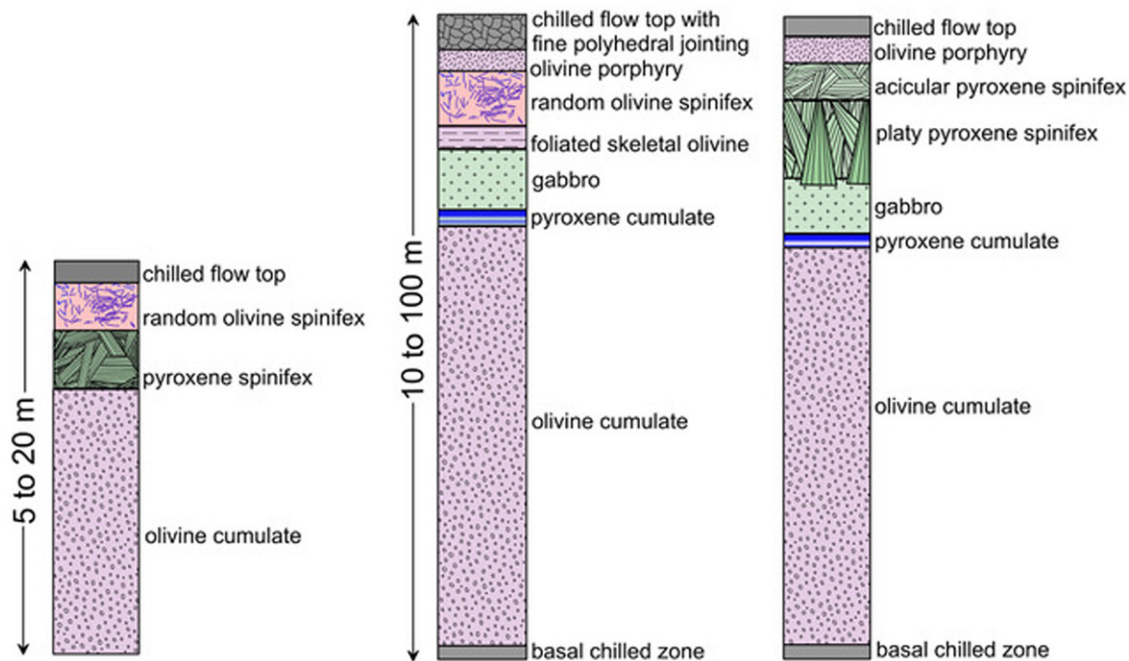


Figure 1. Sketches of three types of komatiite lava flows in the Mashad region.

All samples have experienced varying degrees of hydrothermal alteration and are typically metamorphosed to lower to upper greenschist facies, or to hornblende hornfels facies along the contacts with Triassic Mashhad granitoids. Most of the olivine has been replaced by serpentine, though relicts are

preserved in many samples. Clinopyroxene is largely unaltered, as is chromite but for thin rims of Ti-magnetite. Primary plagioclase is replaced by albite and fine-grained secondary minerals.

The **chilled flow tops** contain abundant (20–50 vol%) small (1–2 mm) phenocrysts

of olivine and sparse clinopyroxene and a few larger phenocrysts, set in a matrix of fine clinopyroxene grains and altered glass. In samples **containing random olivine spinifex texture** (Figs. 2B–2D), 40–60 vol% olivine is set in a matrix of large anhedral to subhedral grains of clinopyroxene, small euhedral chromite

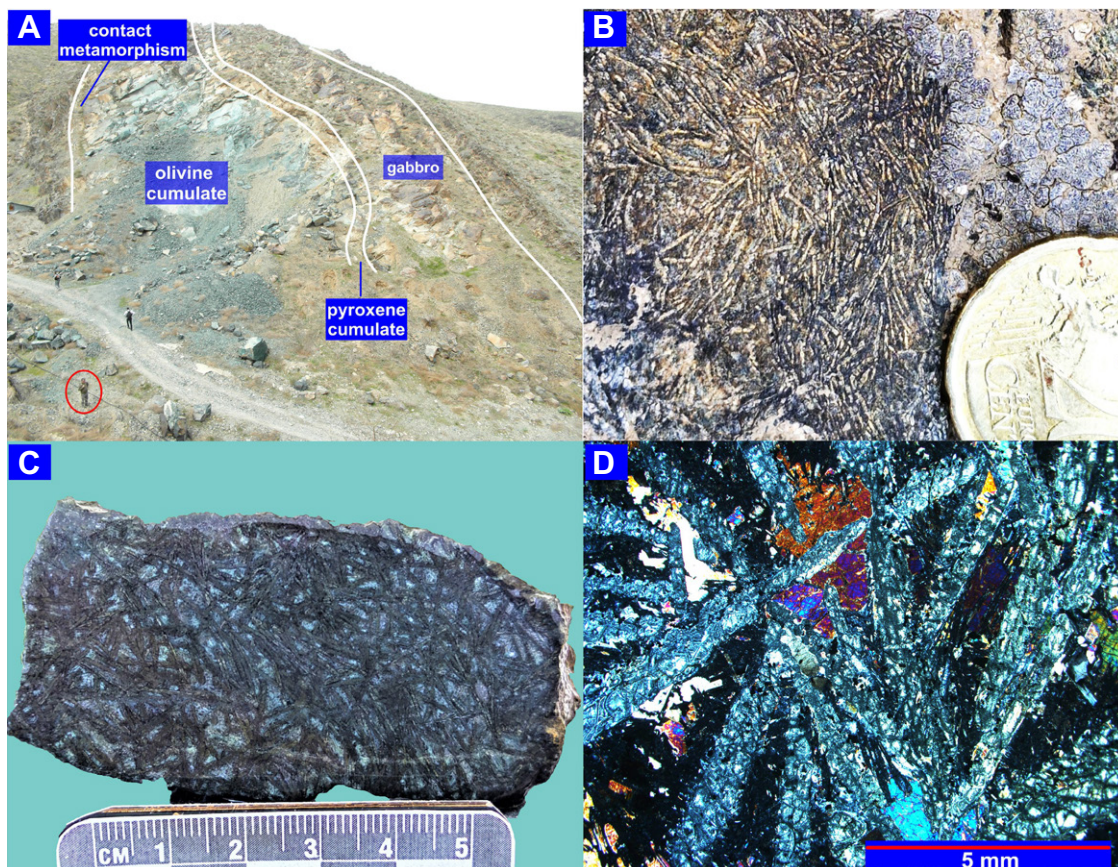


Figure 2. Images illustrating Mashhad komatiites, NE Iran. (A) Field photo of typical differentiated komatiitic basaltic flow. Person highlighted in red circle in lower left for scale. (B, C) Random olivine spinifex texture in the field and in a hand sample. Coin diameter: 2.2 cm. (D) Same texture in thin section (crossed polars).

crystals, and minor magmatic hornblende and altered plagioclase. The randomly oriented olivine crystals are relatively stubby (aspect ratio 5:1) and poorly skeletal (Figs. 2B–2D). They are partially enclosed by unusually large, anhedral grains of clinopyroxene (aluminous diopside). The groundmass consists of fine-grained intergrowths of clinopyroxene, altered plagioclase, and minor brown magmatic hornblende. Altered glass is rare. **Pyroxene spinifex** contains fine-grained (as long as 1.5 mm) randomly oriented crystals or larger needles (5–15 cm) oriented roughly parallel to the flow top. **Gabbros** are medium-grained rocks containing 40–60 vol% euhedral to skeletal clinopyroxene grains and ~30% plagioclase. **Pyroxene cumulates** contain 60–90 vol% coarse poikilitic clinopyroxenes enclosing fine, rounded olivine grains (10–20 vol%). **Olivine cumulates** contain 60–90 vol% olivine grains, usually solid

and polyhedral but in some cases highly skeletal, set in a matrix of coarse clinopyroxene and fine-grained altered plagioclase. Small equant chromite grains and rare hornblende are accessory minerals.

### MINERAL COMPOSITIONS

Representative analyses of the magmatic minerals are given in the Supplemental Material (Table S1), and more complete data are provided in a forthcoming paper (see Supplemental Material). The forsterite content of olivine varies from 85 to 89 [Fo = 100 × Mg/(Mg + Fe) in mol%] in the more mafic units and from 89 to a maximum of 91 in olivine spinifex and the chilled margins of ultramafic units. The clinopyroxene is augite with an unusually high Al<sub>2</sub>O<sub>3</sub> content (2.5–8.8 wt%). Chrome spinel, which is common as inclusions in olivine and as a phenocrysts in the groundmass, contains 15–16 wt%

Al<sub>2</sub>O<sub>3</sub> and 47–50 wt% Cr<sub>2</sub>O<sub>3</sub>, similar to that in other komatiites (Table S2). Phenocrysts of chrome spinel are rimmed by chromium-rich titanomagnetite. Plagioclase, where preserved, contains about 70 mol% anorthite.

### MAJOR AND TRACE ELEMENTS

As shown in Table S3 and Figures 3 and S2, the compositions of the Mashhad lavas vary from ultramafic in the olivine-bearing portions to mafic in gabbroic sections. MgO contents range from 30 to 35 wt% in olivine spinifex, 35–36 wt% in chilled margins, 31–38 wt% in olivine cumulates, and 7–10 wt% in gabbros (Fig. 3; Table S3; Fig. S2). It is notable that the compositions of samples with random olivine textures are similar to those of the olivine cumulates.

In the variation diagrams in Figure 3, most of the data for immobile elements such as Al, Ti, Fe, and Mg in the ultramafic units plot on olivine

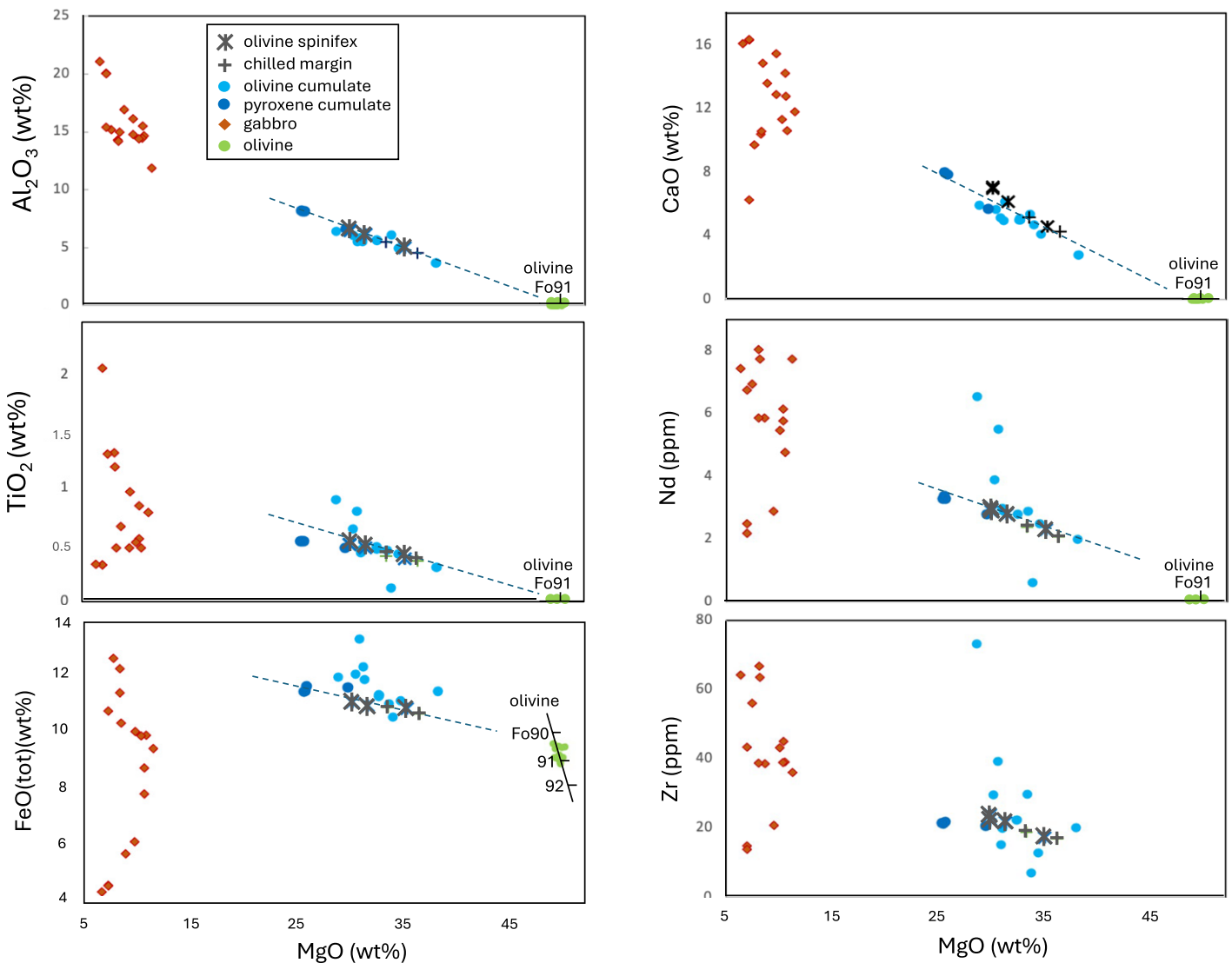


**Figure 3.** Variation diagrams showing the compositions of Mashhad komatiites and those of olivine within chilled margin and olivine spinifex samples [FeO(tot) = <sup>2+</sup>Fe and <sup>3+</sup>Fe expressed as FeO]. Variation within the rock compositions is controlled by the accumulation of olivine with the composition Fo89–90 [Fo = 100 × Mg/(Mg + Fe) in mol%].

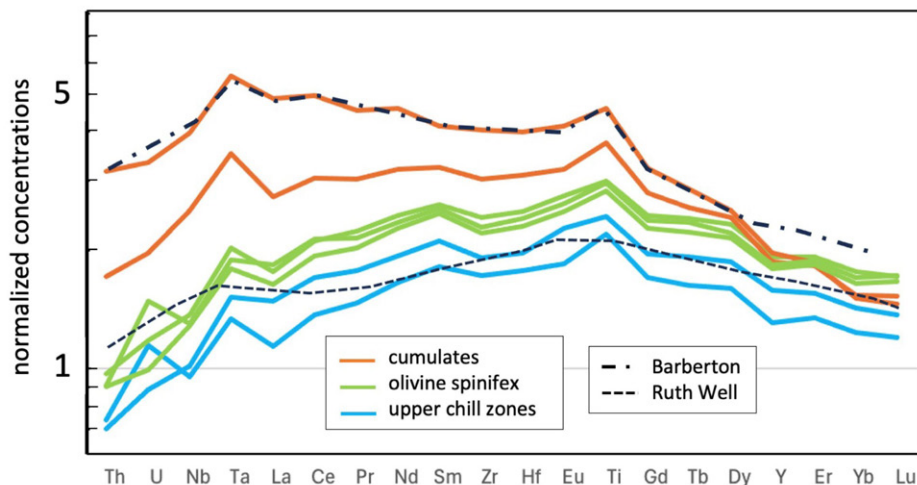


**Figure 4.** Trace-element data, normalized using the primitive mantle values of Hofmann (1988). Note the hump shape resulting from relative depletion of both the more incompatible elements and the heavy rare earth elements. The two cumulates with high concentrations do not come from the same flow as the other samples. Pattern of the cumulates closely resembles that of Archean komatiites from the Barberton Greenstone Belt in South Africa; other samples resemble komatiites from Ruth Well in Australia (data for these samples are from Sossi et al., 2016).

ine control lines. The regression lines on these diagrams indicate that the olivine that controlled the rock compositions had a forsterite content close to 91, similar to that measured with microprobe analyses. Mobile elements such as Na and most trace elements show variable amounts of scatter about these lines. Some samples have elevated contents of  $\text{TiO}_2$  and most incompatible trace elements and probably come from another magma source.

The  $\text{Al}_2\text{O}_3/\text{TiO}_2$  values of these komatiites range from  $\sim 10$  to 12 (or 6–7 in the samples with elevated  $\text{TiO}_2$  contents); this indicates that these rocks belong to the Al-depleted type of komatiite (Nesbitt et al., 1979). This is substantiated by the mantle-normalized trace element patterns, plotted in Figure 4, which show the relative depletion of heavy rare earth elements that characterizes this type of komatiite. The hump shape resembles that of komatiites from localities such as Ruth Well in Australia (Nisbet and Chinner, 1981) and in Finnish Lapland (Hanski et al., 2001).

## DISCUSSION

### Ultramafic Character of Mashhad Komatiites

The presence of random olivine spinifex textures in the Mashhad komatiites distinguishes them from all other post-Archean ultramafic lavas with the exception of the Gorgona Island komatiites (Echeverría, 1980) and the Gilmour Island komatiitic basalts (Arndt et al., 1987). The MgO contents of the Mashhad ultramafic rocks exceed 20 wt%, and this, together with the spinifex textures, leaves no doubt as to their komatiitic character.

The MgO contents, and hence the eruption temperatures, of komatiites are normally esti-

mated using several complementary approaches based on the compositions of whole rocks and preserved olivines (Nisbet et al., 1993; Waterton and Arndt, 2024). The first is to use the composition of samples with random spinifex textures because these are assumed to result from rapid cooling and crystallization under conditions in which olivine does not accumulate (Nesbitt, 1971). Samples of Mashhad komatiites with olivine spinifex textures have unusually high MgO contents, from 30 to 35 wt%, values that approach or exceed those of the most magnesian Archean komatiites.

The second approach is to use the composition of the most magnesian olivine in the samples and the Mg-Fe distribution coefficient (Bickle, 1982). In the Mashhad samples, the most magnesian olivine composition recorded in the electron microprobe analyses is Fo91, a value consistent with the olivine compositions estimated from the variation diagrams (Fig. 3). For dry conditions at 1 kbar pressure and at the QFM (quartz-fayalite-magnetite) buffer, Ford et al.'s (1983) model for olivine fractionation of the least MgO-rich random spinifex sample (FC-5) predicts 20 wt% MgO in a melt in equilibrium with olivine Fo91. The MgO value falls at the limit between komatiite and komatiitic basalt and, remarkably, is far lower than the MgO contents of the olivine spinifex samples (30–35 wt%).

Several other observations support the conclusion that the parental liquid did not have the high MgO content of the olivine spinifex samples: (1) The mineral assemblage interstitial to olivine in both spinifex-textured and cumulate samples consists of abundant clinopyroxene and chrome spinel and accessory plagioclase and hornblende. This assemblage resembles that

of a komatiitic basalt rather than a komatiite. (2) Some olivine grains contain inclusions of chromite. (3) In a MgO versus Cr diagram (Fig. S3), the whole-rock compositions plot about a line with a positive slope indicating co-crystallization of olivine and chrome spinel. The latter mineral crystallizes only in magmas with  $< \sim 25$  wt% MgO (Murck and Campbell, 1986).

An additional method to infer the MgO content and eruption temperature of the komatiite melt comes from geothermometry. As shown in Figure S4, we estimate a temperature of 1460 °C using olivine (Fo90.2) and co-existing spinel and the method of Wan et al. (2008). This temperature would normally correspond to olivine with a higher forsterite content, Fo92, which would have crystallized from an anhydrous melt containing  $\sim 22$  wt% MgO. The presence of amphibole suggests, however, that the melt contained some water. If it contained 0.5 wt% water, as recorded in other komatiites (Sobolev et al., 2019), the original olivine would have had the composition Fo94, and the MgO content in the equilibrium melt would have been  $\sim 25$  wt% (Fig. S4). The mismatch between measured and predicted forsterite contents may indicate that the olivine partly re-equilibrated with melt at lower temperature.

On the basis of these observations, together with the estimates based on the olivine compositions, we conclude that the Mashhad komatiites crystallized from melts with an MgO content of at least 21–22 wt%, slightly lower than that of komatiites and picrites from Gorgona Island but higher than values in other post-Archean komatiites. We do not have a ready explanation for the unusually high MgO contents of the olivine spinifex samples. We note, however, that the olivine crystals have a morphology different from those in Archean olivine spinifex, being stubbier and only marginally skeletal. Fine, highly elongate dendritic crystals like those in Archean komatiites are absent. We also note the high concentration, as much as 50%, of fine olivine phenocrysts in the chilled margins and speculate that spinifex olivines in Mashhad komatiites nucleated around these crystals. The addition of up to 50% accumulated olivine could explain the elevated MgO in the spinifex samples.

This result indicates that caution must be applied when using the compositions of spinifex-textured samples to estimate the melt composition. In many komatiite suites, the compositions of rocks with random olivine spinifex textures do indeed resemble the melt compositions inferred from the forsterite contents of olivine. Examples include suites from Barberton Greenstone Belt in South Africa (Parman et al., 1997), Alexo in Canada (Arndt, 1986), and Gorgona Island (Echeverría, 1980). In such examples, the approach is sound, but the discrepancy noted in the Mashhad samples shows that this is not always the case.

## Origin of Mashhad Komatiites

Another feature that distinguishes these komatiites from all other post-Archean examples is their Al-depleted character. This, together with the relative depletion of the heavy rare earth elements (Fig. 4), indicates that garnet was a residual phase at some stage of their formation (Green, 1975; Jahn et al., 1982). In addition, the relative depletion of the light rare earth elements points to a source depleted in the more incompatible elements. Using the approach described by Waterton and Arndt (2024), Ti can be assumed to behave incompatibly and provides an estimate of the degree of melting. Taking a TiO<sub>2</sub> content of 0.8% in a melt with 20% MgO (from the MgO versus TiO<sub>2</sub> diagram, Fig. 3) and assuming a depleted mantle source containing 0.13% TiO<sub>2</sub> (Salters and Stracke, 2004), we estimate ~20% partial melting.

To estimate the conditions of partial melting, we use the phase diagram for mantle peridotite (Fig. S5) and the following constraints: 22 wt% MgO in the primary melt and 20% partial melting in the presence of garnet. Reference to Figure S5 shows that the primary melt could not have been produced from dry peridotite because if the melt is in the field of garnet stability, the MgO content is too high and the degree of melting is too low. The presence of amphibole and phlogopite in the Mashhad komatiites suggests, however, that the source contained a small content of H<sub>2</sub>O. Melting of such a source at ~6 GPa (~180 km depth) and a temperature ~1600 °C could have produced a melt of appropriate composition. Given the uncertainty about the position of the solidus and garnet stability curve, the conditions of melting cannot be determined with better precision (numerical approaches such as that proposed by Lee and Chin [2014] do not apply to melting of hydrous peridotite).

## ACKNOWLEDGMENTS

This project received funding from the European Research Council under the European Union's Horizon 2020 program (grant agreement 856555). We thank Steve Barnes, Pedro Waterton, Euan Nisbet, and Allan Wilson for helpful discussions and Mike Lesher, Derek Wyman, and Robert Bolhar for constructive reviews.

## REFERENCES CITED

Arndt, N.T., 1986, Differentiation of komatiite flows: *Journal of Petrology*, v. 27, p. 279–301, <https://doi.org/10.1093/ptrology/27.2.279>.

Arndt, N.T., Brüggmann, G.E., Lehnert, K., Chauvel, C., and Chappell, B.W., 1987, Geochemistry, petrogenesis and tectonic environment of Circum-Superior Belt basalts, Canada, in Pharaoh, T.C., et al., eds., *Geochemistry and Mineralization of Proterozoic Volcanic Suites*: Geological Society, London, Special Publication 33, p. 133–145, <https://doi.org/10.1144/GSL.SP.1987.033.01.10>.

Bickle, M.J., 1982, The magnesium content of komatiitic liquids, in Arndt, N.T., and Nisbet, E.G., eds., *Komatiites*: London, George Allen and Unwin, p. 479–494.

Echeverría, L.M., 1980, Tertiary or Mesozoic komatiites from Gorgona Island, Colombia: Field relations and geochemistry: *Contributions to Mineralogy and Petrology*, v. 73, p. 253–266, <https://doi.org/10.1007/BF00381444>.

Ford, C.E., Russell, D.G., Craven, J.A., and Fisk, M.R., 1983, Olivine-liquid equilibria: Temperature, pressure and composition dependence of the crystal/liquid cation partition coefficients for Mg, Fe<sup>2+</sup>, Ca and Mn: *Journal of Petrology*, v. 24, p. 256–266, <https://doi.org/10.1093/ptrology/24.3.256>.

Ghazi, A.M., Hassani, A.A., Tucker, P.J., Mobasher, K., and Duncan, R.A., 2001, Geochemistry and <sup>40</sup>Ar–<sup>39</sup>Ar ages of the Mashhad Ophiolite, NE Iran: A rare occurrence of a 300 Ma (Paleo-Tethys) oceanic crust: *Eos (Transactions, American Geophysical Union)*, v. 82, no. 47, Fall Meeting suppl., abstract V12C-0993.

Green, D.H., 1975, Genesis of Archean peridotitic magmas and constraints on Archean geothermal gradients and tectonics: *Geology*, v. 3, p. 15–18, [https://doi.org/10.1130/0091-7613\(1975\)3<15:GOAPMA>2.0.CO;2](https://doi.org/10.1130/0091-7613(1975)3<15:GOAPMA>2.0.CO;2).

Hanski, E., Huhma, H., Rastas, P., and Kamenitsky, V.S., 2001, The Palaeoproterozoic komatiite–picrite association of Finnish Lapland: *Journal of Petrology*, v. 42, p. 855–876, <https://doi.org/10.1093/ptrology/42.5.855>.

Hanski, E., Walker, R.J., Huhma, H., Polyakov, G.V., Balykin, P.A., Hoa, T.T., and Phuong, N.T., 2004, Origin of the Permian–Triassic komatiites, northwestern Vietnam: *Contributions to Mineralogy and Petrology*, v. 147, p. 453–469, <https://doi.org/10.1007/s00410-004-0567-1>.

Hofmann, A.W., 1988, Chemical differentiation of the Earth: The relationship between mantle, continental crust, and oceanic crust: *Earth and Planetary Science Letters*, v. 90, p. 297–314, [https://doi.org/10.1016/0012-821X\(88\)90132-X](https://doi.org/10.1016/0012-821X(88)90132-X).

Jahn, B.-M., Gruau, G., and Glikson, A.Y., 1982, Komatiites of the Onverwacht Group, S. Africa: REE geochemistry, Sm/Nd age and mantle evolution: *Contributions to Mineralogy and Petrology*, v. 80, p. 25–40, <https://doi.org/10.1007/BF00376732>.

Kerr, A.C., 2005, La Isla de Gorgona, Colombia: A petrological enigma?: *Lithos*, v. 84, p. 77–101, <https://doi.org/10.1016/j.lithos.2005.02.006>.

Kozur, H., and Mostler, H., 1991, Pelagic Permian conodonts from an oceanic sequence at Sang-e-Sefid (Fariman, NE-Iran), in Ruttner, A.W., ed., *The Triassic of Aghdarband (AqDarband), NE-Iran, and its Pre-Triassic Frame*: Vienna, Federal Geological Institute, v. 38, p. 101–110.

Lee, C.-T.A., and Chin, E.J., 2014, Calculating melting temperatures and pressures of peridotite protoliths: Implications for the origin of cratonic mantle: *Earth and Planetary Science Letters*, v. 403, p. 273–286, <https://doi.org/10.1016/j.epsl.2014.06.048>.

Mobasher, M., Garrido, C.J., Ghasemi, H., Marchesi, C., Rahimi, B., Hidas, K., and Gourabjri-Pour, A., 2019, Field evidence and geochemistry of komatiites from the Shandiz-Virani Mashhad Complex, Northeast Iran: Abstract presented at 28th Goldschmidt Conference, Barcelona, 18–23 August, <https://hdl.handle.net/10261/207869>.

Murck, B.W., and Campbell, I.H., 1986, The effects of temperature, oxygen fugacity and melt composition on the behaviour of chromium in basic and ultrabasic melts: *Geochimica et Cosmochimica Acta*, v. 50, p. 1871–1887, [https://doi.org/10.1016/0016-7037\(86\)90245-0](https://doi.org/10.1016/0016-7037(86)90245-0).

Nesbitt, R.W., 1971, Skeletal crystal forms in the ultramafic rocks of the Yilgarn Block, Western Australia: Evidence for an Archean ultramafic liquid: *Geological Society of Australia Special Publications*, v. 3, p. 331–347.

Nesbitt, R.W., Sun, S.-S., and Purvis, A.C., 1979, Komatiites: Geochemistry and genesis: *Canadian Mineralogist*, v. 17, p. 165–186.

Nesbitt, R.W., Jahn, B.M., and Purvis, A.C., 1982, Komatiites: An early Precambrian phenomenon: *Journal of Volcanology and Geothermal Research*, v. 14, p. 31–45, [https://doi.org/10.1016/0377-0273\(82\)90041-5](https://doi.org/10.1016/0377-0273(82)90041-5).

Nisbet, E.G., and Chinner, G.A., 1981, Controls of the eruption of mafic and ultramafic lavas, Ruth Well Ni-Cu prospect, West Pilbara: *Economic Geology*, v. 76, p. 1729–1735, <https://doi.org/10.2113/gsecongeo.76.6.1729>.

Nisbet, E.G., Cheadle, M.J., Arndt, N.T., and Bickle, M.J., 1993, Constraining the potential temperature of the Archean mantle: A review of the evidence from komatiites: *Lithos*, v. 30, p. 291–307, [https://doi.org/10.1016/0024-4937\(93\)90042-B](https://doi.org/10.1016/0024-4937(93)90042-B).

Parman, S.W., Dann, J.C., Grove, T.L., and de Wit, M.J., 1997, Emplacement conditions of komatiite magmas from the 3.49 Ga Komati Formation, Barberton Greenstone Belt, South Africa: *Earth and Planetary Science Letters*, v. 150, p. 303–323, [https://doi.org/10.1016/S0012-821X\(97\)00104-0](https://doi.org/10.1016/S0012-821X(97)00104-0).

Salters, V.J.M., and Stracke, A., 2004, Composition of the depleted mantle: *Geochemistry, Geophysics, Geosystems*, v. 5, Q05B07, <https://doi.org/10.1029/2003GC000597>.

Sobolev, A.V., Asafov, E.V., Gurenko, A.A., Arndt, N.T., Batanova, V.G., Portnyagin, M.V., Garbe-Schönberg, D., Wilson, A.H., and Byerly, G.R., 2019, Deep hydrous mantle reservoir provides evidence for crustal recycling before 3.3 billion years ago: *Nature*, v. 571, p. 555–559, <https://doi.org/10.1038/s41586-019-1399-5>.

Sossi, P.A., Eggins, S.M., Nesbitt, R.W., Nebel, O., Hergt, J.M., Campbell, I.H., O'Neill, H.S.C., Kranendonk, M.V., and Rhodri Davies, D., 2016, Petrogenesis and geochemistry of Archean komatiites: *Journal of Petrology*, v. 57, p. 147–184, <https://doi.org/10.1093/ptrology/egw004>.

Topuz, G., Hegner, E., Homam, S.M., Ackerman, L., Pfänder, J.A., and Karimi, H., 2018, Geochemical and geochronological evidence for a Middle Permian oceanic plateau fragment in the Paleoproterozoic suture zone of NE Iran: *Contributions to Mineralogy and Petrology*, v. 173, 81, <https://doi.org/10.1007/s00410-018-1506-x>.

Trela, J., Gazel, E., Sobolev, A.V., Moore, L., Bizimis, M., Jicha, B., and Batanova, V.G., 2017, The hottest lavas of the Phanerozoic and the survival of deep Archean reservoirs: *Nature Geoscience*, v. 10, p. 451–456, <https://doi.org/10.1038/ngeo2954>.

Wan, Z., Coogan, L., and Canil, D., 2008, Experimental calibration of aluminum partitioning between olivine and spinel as a geothermometer: *American Mineralogist*, v. 93, p. 1142–1147, <https://doi.org/10.2138/am.2008.2758>.

Waterton, P., and Arndt, N., 2024, Komatiites: Their geochemistry and origins, in Homann, M., et al., *The Archean Earth: Tempos and Events* (2nd edition): Elsevier (in press).

Zanchetta, S., Berra, F., Zanchi, A., Bergomi, M., Caridroit, M., Nicora, A., and Heidarzadeh, G., 2013, The record of the Late Palaeozoic active margin of the Palaeotethys in NE Iran: Constraints on the Cimmerian orogeny: *Gondwana Research*, v. 24, p. 1237–1266, <https://doi.org/10.1016/j.gr.2013.02.013>.

Printed in the USA